



Universiteit
Leiden
The Netherlands

A genetic interaction map centered on cohesin reveals auxiliary factors involved in sister chromatid cohesion in *S. cerevisiae*

Sun, S.M.; Batte, A.; Elmer, M.; Horst, S.C. van der; Welsem, T. van; Bean, G.; ... ; Attikum, H. van

Citation

Sun, S. M., Batte, A., Elmer, M., Horst, S. C. van der, Welsem, T. van, Bean, G., ... Attikum, H. van. (2020). A genetic interaction map centered on cohesin reveals auxiliary factors involved in sister chromatid cohesion in *S. cerevisiae*. *Journal Of Cell Science*, 133(10).
doi:10.1242/jcs.237628

Version: Publisher's Version
License: [Creative Commons CC BY 4.0 license](https://creativecommons.org/licenses/by/4.0/)
Downloaded from: <https://hdl.handle.net/1887/3184389>

Note: To cite this publication please use the final published version (if applicable).

RESEARCH ARTICLE

A genetic interaction map centered on cohesin reveals auxiliary factors involved in sister chromatid cohesion in *S. cerevisiae*

Su Ming Sun^{1,*}, Amandine Batté^{1,*}, Mireille Elmer^{1,2}, Sophie C. van der Horst¹, Tibor van Welsem³, Gordon Bean⁴, Trey Ideker^{4,5,6,7}, Fred van Leeuwen³ and Haico van Attikum^{1,‡}

ABSTRACT

Eukaryotic chromosomes are replicated in interphase and the two newly duplicated sister chromatids are held together by the cohesin complex and several cohesin auxiliary factors. Sister chromatid cohesion is essential for accurate chromosome segregation during mitosis, yet has also been implicated in other processes, including DNA damage repair, transcription and DNA replication. To assess how cohesin and associated factors functionally interconnect and coordinate with other cellular processes, we systematically mapped the genetic interactions of 17 cohesin genes centered on quantitative growth measurements of >52,000 gene pairs in the budding yeast *Saccharomyces cerevisiae*. Integration of synthetic genetic interactions unveiled a cohesin functional map that constitutes 373 genetic interactions, revealing novel functional connections with post-replication repair, microtubule organization and protein folding. Accordingly, we show that the microtubule-associated protein Irc15 and the prefoldin complex members Gim3, Gim4 and Yke2 are new factors involved in sister chromatid cohesion. Our genetic interaction map thus provides a unique resource for further identification and functional interrogation of cohesin proteins. Since mutations in cohesin proteins have been associated with cohesinopathies and cancer, it may also help in identifying cohesin interactions relevant in disease etiology.

KEY WORDS: Genetic interaction mapping, Cohesin, Sister chromatid cohesion, Prefoldin, Irc15, Cohesinopathy

INTRODUCTION

Sister chromatid cohesion ensures close proximity of the two sister chromatids from the time of replication until their separation to opposite spindle poles during mitosis. Sister chromatid cohesion is

mediated in all eukaryotic cells by a multiprotein complex called cohesin (Michaelis et al., 1997). In budding yeast (*Saccharomyces cerevisiae*), Smc1, Smc3, Scc1 and Scc3 make up the core of the cohesin complex, which is loaded onto chromatin during G1 phase. It forms a ring-like structure that encircles sister chromatids generated during DNA replication in S phase in a manner dependent on Smc3 acetylation by Eco1. Subsequently the cohesive status is sustained throughout G2 and M phase by several maintenance factors, including Rad61, Pds5 and Sgo1. Several accessory proteins have also been implicated in promoting sister chromatid cohesion, including Elg1, Ctf18, the alternative replication factor C (RFC) complexes, the replisome component Ctf4, the Chl1 helicase-like protein, the chromatin remodeler Chd1 and the S phase checkpoint proteins Mrc1 and Tof1 (Petronczki et al., 2004; Parnas et al., 2009; Hanna et al., 2001; Skibbens, 2004; Xu et al., 2004; Boginya et al., 2019). Finally, sister chromatid cohesion is dissolved at the metaphase to anaphase transition by proteolytic activity of Esp1 towards Scc1 (Uhlmann et al., 1999; Cohen-Fix et al., 1996; Xiong and Gerton, 2010).

Besides ensuring proper chromosome segregation, cohesin has been shown to impact the repair of DNA double-strand breaks (DSBs) (Unal et al., 2004, 2007; Strom et al., 2004; Heidinginger-Pauli et al., 2009; Gelot et al., 2016; Wu et al., 2012; Kong et al., 2014), gene expression (Gullerova and Proudfoot, 2008; Dorsett, 2011; Lengronne et al., 2004) and nuclear organization (Harris et al., 2014; Yamin et al., 2020). In addition, several developmental disorders have been causally linked to germline mutations in cohesin genes and are collectively referred to as cohesinopathies. These include Cornelia de Lange syndrome (Deardorff et al., 2012; Liu and Baynam, 2010), Roberts syndrome (Vega et al., 2005) and Warsaw breakage syndrome (van der Lelij et al., 2010). Somatic mutations in cohesin genes, on the other hand, have been found with high frequency in various types of cancer (Thol et al., 2014; Bailey et al., 2014; Repo et al., 2016; Deb et al., 2014), underscoring the importance of cohesin genes in the development of pathogenesis. However, despite the important role that cohesin genes play in various cellular processes, including those relevant to disease manifestation, our understanding of how the cohesin complex functionally interconnects with these processes is still rather limited.

Genetic interaction screens have highlighted the connectivity between genes and their corresponding pathways, thus providing insight into the biological role(s) of individual genes (Mani et al., 2008). In yeast, such screens have led to the identification of new genes that contribute to efficient sister chromatid cohesion (Mayer et al., 2004; Chen et al., 2012), and provided valuable insight into the connectivity between cohesin genes and genes involved in DNA repair and DNA replication (McLellan et al., 2012; Warren et al., 2004). However, these studies were focused on a rather limited number of cohesin genes. Here, we examined genetic interactions between 17 different cohesin genes and more than 1400 genes

¹Department of Human Genetics, Leiden University Medical Center, Einthovenweg 20, 2333 ZC, Leiden, Netherlands. ²Electrical Engineering, Mathematics and Computer Science, Delft University of Technology, 2600 AA, Delft, Netherlands.

³Division of Gene Regulation, Netherlands Cancer Institute, Plesmanlaan 121, 1066 CX, Amsterdam, Netherlands. ⁴Bioinformatics and Systems Biology Program, University of California, San Diego, La Jolla, CA, 92093, USA. ⁵Department of Medicine, Division of Genetics, University of California, San Diego, La Jolla, CA, 92093, USA. ⁶Department of Bioengineering, University of California, San Diego, La Jolla, CA, 92093, USA. ⁷Cancer Cell Map Initiative (CCMI), Moores UCSD Cancer Center, La Jolla, CA, 92093, USA.

*These authors contributed equally to this work

‡Author for correspondence (h.van.attikum@umc.nl)

DOI: 10.1242/jcs.237628; T.I., 0000-0002-1708-8454; F.v.L., 0000-0002-7267-7251; H.v.A., 0000-0001-8590-0240

This is an Open Access article distributed under the terms of the Creative Commons Attribution License (<https://creativecommons.org/licenses/by/4.0>), which permits unrestricted use, distribution and reproduction in any medium provided that the original work is properly attributed.

Handling Editor: David Glover

Received 7 August 2019; Accepted 26 March 2020

involved in various biological processes in a quantitative manner. The resulting genetic interaction map describes novel connections for cohesin genes in various cellular processes, including post-replication repair, microtubule organization and protein folding, and reveals that the microtubule-associated protein Irc15 and prefoldin complex members Gim3, Gim4 and Yke2 are novel regulators of sister chromatid cohesion. Thus, we provide a unique and powerful resource for the identification and functional interrogation of cohesin proteins.

RESULTS

Mapping genetic interactions of cohesin

To gain more insight into the relationship between sister chromatid cohesion and other cellular processes, a comprehensive genetic interaction map centered on cohesin was generated. To this end, query strains carrying gene deletion or temperature-sensitive alleles of 17 different cohesin genes and 18 DNA damage response (DDR) genes (Table S1) were crossed by using the synthetic genetic array (SGA) methodology (Tong and Boone, 2006) against a panel of 1494 array strains (Table S2) carrying gene deletion or decreased abundance of mRNA perturbation (DAmP) alleles of genes that represent various biological processes (Fig. 1A). We previously used the 18 DDR mutants to map interactions of the DDR network,

and included these in the current study to warrant quality control and quality assurance (Guenole et al., 2013; Srivas et al., 2013). Genetic interactions were scored by quantifying colony sizes of the double mutants, which were normalized and statistically analyzed to provide each mutant with a quantitative S-score (Fig. 1A). S-scores ≤ -2.5 represent negative or synthetic sick/lethal interactions, whereas S-scores ≥ 2 represent positive or alleviating/repressive interactions (Costanzo et al., 2019; St Onge et al., 2007; Hartman et al., 2001). In total, the profile map contains S-scores for 52,290 gene pairs (Fig. 1A; Table S3). Several routine quality control metrics were employed to ensure a high-quality map (Fig. S1). We observed a correlation of at least 50% between the genetic interactions identified in our screen and previously published genetic interaction maps (Fig. S1A,B) (Guenole et al., 2013; Collins et al., 2010; Costanzo et al., 2010). In addition, genetic interactions with the highest S-scores showed a high enrichment of interactions present in the Biogrid database (Fig. S1C).

Our genetic interaction map revealed in total 678 interactions, including 55 positive and 632 negative interactions (Fig. 1B). Validation of ~ 70 interactions resulted in an overall false discovery rate (FDR) of 31% (Fig. S1D–G). In particular, we identified 348 negative and 25 positive interactions for the cohesin-related genes along with 342 negative and 33 positive interactions for the DDR

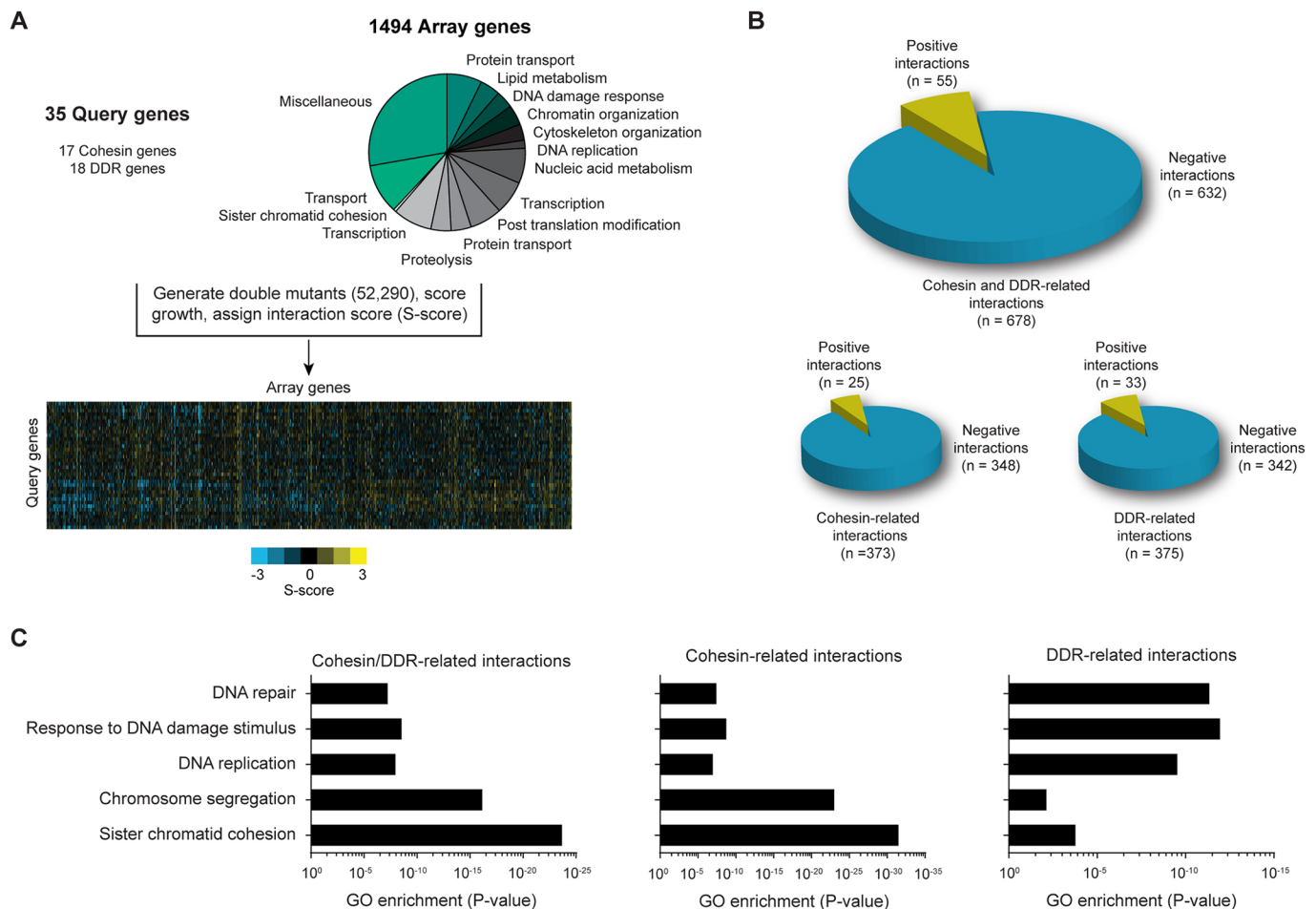


Fig. 1. A genetic interaction map centered on cohesin. (A) Outline of the genetic interaction screen. Mutants in 17 cohesin and 18 DNA damage response (DDR) query genes were crossed against a panel of 1494 mutants in array genes involved in various biological processes. Genetic interactions were scored by quantification of colony sizes, providing each double mutant with a quantitative S-score. (B) Total number of positive (S-score ≥ 2) and negative (S-score ≤ -2.5) interactions for all query (top), cohesin (bottom left) or DDR (bottom right) genes. (C) GO term enrichment of interactions involving all (left), cohesin (middle) or DDR genes (right).

genes (Fig. 1B). As expected, interactions found in the cohesin-associated group were highly enriched for the Gene Ontology (GO) terms ‘sister chromatid cohesion’ and ‘chromosome segregation’, whereas interactions for the DDR-associated genes were enriched for DNA repair-related GO terms (Fig. 1C; Tables S4–S6). In conclusion, a high-quality genetic interaction map centered on cohesin was generated, providing a useful resource to mine for crosstalk between sister chromatid cohesion and other cellular processes.

Cohesin genes interconnect with genes involved in various biological processes

To better understand the complexity of the interplay between sister chromatid cohesion and other biological processes, we generated a

genetic interaction network comprising interactions with S-scores ≤ -2.5 and ≥ 2 for the cohesin-related query genes (Fig. 2). This interaction network may be relevant for other species as the vast majority of genes are orthologous to both fission yeast and human genes (Table S7).

As expected, we observed a strong relationship between sister chromatid cohesion factors and genes involved in cell cycle control (e.g. *SIC1*, *CTF19*, *BUB1* and *BUB3*), as well as in DNA replication (e.g. *RTT101*, *MMS22* and *POL2*), which is in agreement with the required coordination of these three processes to guarantee faithful chromosome duplication and segregation (Lengronne and Schwob, 2002; Fernius and Marston, 2009; Alexandru et al., 1999; Zhang et al., 2017; Edwards et al., 2003). Our network also revealed

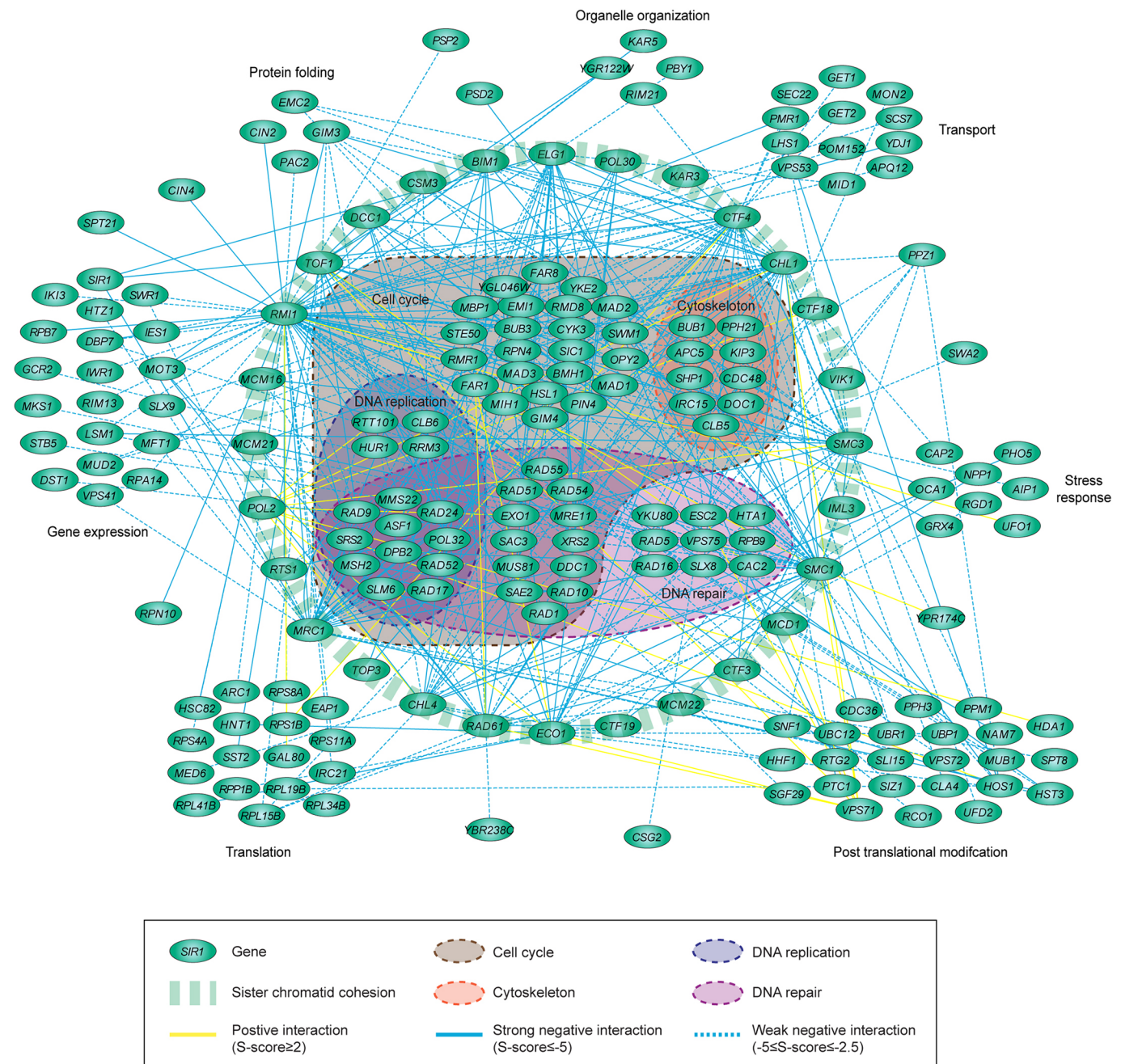


Fig. 2. A genetic interaction network centered on cohesin. Visualization of significant genetic interactions of cohesin-related genes. Interacting genes were grouped based on GO annotation.

several known interactions between cohesin factors, mainly the non-essential cohesin accessory factors, such as *ELG1*, *TOF1* and *RMII*, and genes involved in DSB repair (e.g. *RAD51*, *RAD52* and *SRS2*) (Ben-Aroya et al., 2003; Chang et al., 2005; Kanellis et al., 2003). Moreover, several interactions between cohesin factors and chromatin remodeling or histone-modifying complexes, such as *ASF1*, *IES1*, *HTZ1*, *SWR1*, *HDA1* and *HST3*, strengthen the link between sister chromatin cohesion and chromatin architecture (Huang et al., 2004; Huang and Laurent, 2004; Munoz et al., 2019; Sharma et al., 2013; Thamiy et al., 2007). Finally, we found a strong interplay between both essential and non-essential cohesin genes and genes encoding ribosomal subunits such as *RPL15B*, *RPBL41B* and *RPBL19B*. This is consistent with recent findings showing that defects in cohesin genes lead to defects in the production of ribosomal RNA and translation efficacy in both budding yeast and patient cells (Sun et al., 2015; Bose et al., 2012; Xu et al., 2014; Lu et al., 2014).

Our network also revealed several unanticipated interactions (Fig. 2). For example, several interactions between cohesin factors and genes involved in nucleotide excision repair, such as *RAD16* and *RAD1* with *SMC1* and *RAD10* with *RAD61*, in mismatch repair, such as *MSH2* with *MDC1* and *RAD61*, or in template switching, such as *RAD5* with *DCC1* and *RMII*, might indicate a novel role for cohesin in post-replication repair. Supporting this notion, the separase complex is required for cohesin dissociation during post-replicative DNA repair (Nagao et al., 2004; McAleenan et al., 2013). Moreover, *Smc1* is phosphorylated in an ATR-dependent manner after exposure to ultraviolet (UV)-induced DNA damage and the *smc1-259* mutant shows a high sensitivity to UV (Garg et al., 2004; Kim et al., 2002). Finally, several other unanticipated interactions were found between cohesin factors and genes involved in microtubule organization and protein folding, highlighting potential novel functional connections. Taken together, our genetic interaction map provides a resource of known as well as novel interactions between cohesin and genes involved in various biological processes, which may serve as a starting point for unraveling cohesin functions in these processes.

Irc15 promotes the loading of centromeric cohesin

The cohesin interaction network may not only reveal new connections between cohesin genes and distinct biological processes, but may also uncover new factors involved in sister chromatid cohesion. Since genes acting in the same pathway tend to have similar genetic interaction profiles, we employed unsupervised hierarchical clustering of genetic interactions involving both cohesin and DDR-related query genes (Fig. 3A, left panel). Strikingly, a cluster of array genes interacted specifically with the cohesin query genes, which clustered separately from the DDR query genes (Fig. 3A, right panel). Interestingly, within this cluster, genes implicated in the establishment of pericentromeric cohesion, namely *CTF19*, *IML3* and *CHL4*, clustered together but did not interact with the three non-essential cohesin factors *MRC1*, *TOF1* and *ELG1*. While this cluster furthermore included genes implicated in chromosome segregation (e.g. *BIMI*, *MAD2* and *BUB1*), it was mostly dominated by genes involved in sister chromatid cohesion. Interestingly, among the genes in this cluster were also four genes, *GIM4*, *GIM3* and *YKE2*, that were all members of the prefoldin complex, and *IRC15*, a microtubule-binding protein, whose role in this process was unknown. We confirmed the negative genetic interactions of *gim3Δ*, *yke2Δ* and *irc15Δ* with *smc3-1*, and of *gim4Δ* and *yke2Δ* with *smc1-249* at semi-permissive temperature (Fig. S2). To assess their role in sister chromatid cohesion, we first examined

whether *GIM4*, *GIM3*, *YKE2* and *IRC15* affect the loading of cohesin onto chromosomes. *PAC10*, which encodes another member of the prefoldin complex, did not display any significant negative interaction with cohesin genes and was therefore included as a negative control. *Scc1* loading was assessed by chromatin immunoprecipitation (ChIP) at known cohesin-binding sites in G2 cells (Fig. 3B,C). A region on chromosome III devoid of *Scc1* was used as a negative control (Pal et al., 2018). *Scc1* loading was comparable in wild-type (WT) cells and cells lacking *GIM3*, *GIM4*, *YKE2* or *PAC10*, suggesting that the prefoldin complex is not involved in cohesin loading. However, *Scc1* levels were decreased at centromeric regions in the absence of *IRC15*, while they were increased on chromosome arms, indicating that *Irc15* regulates the distribution of cohesin on chromosomes. The defect in centromeric cohesin loading in *irc15Δ* may stem from a translocation of cohesin from the centromeres to the chromosome arms. However, we could not detect any such translocation of *Scc1* by ChIP when cells proceeded from G1 phase to G2/M phase (Fig. S3A–F). Thus, we identify *Irc15* as a new factor involved in the loading of centromeric cohesin. Interestingly, *irc15Δ* cells present a delayed pre-anaphase mitotic entry due to defective kinetochore–microtubule attachments (Keyes and Burke, 2009). Potentially, reduced cohesin loading and, consequently, impaired sister chromatid cohesion may have affected the maintenance of kinetochore–microtubule attachments during mitosis. To address this, we examined whether overexpression of *Scc1* could rescue the kinetochore assembly defects observed in the absence of *IRC15* (Keyes and Burke, 2009). To this end, we monitored binding of the kinetochore-associated *Ndc80* complex, which is involved in kinetochore assembly (McClelland et al., 2003), by performing ChIP of GFP-tagged *Ndc80* at four different centromeres (*CEN2*, *CEN3*, *CEN4* and *CEN8*) and a negative control locus (*Neg1p2*) (Lefrancois et al., 2013) in WT and *irc15Δ* strains carrying a galactose-inducible allele of *SCC1* (Fig. S3G). We found that *Ndc80* binding was increased ~4-fold in the absence of *IRC15* (Fig. S3H), indicative of a kinetochore assembly problem and agreeing with a previous observation (Keyes and Burke, 2009). Importantly, *Ndc80* binding was not affected by *Scc1* overexpression (Fig. S3H), suggesting that reduced cohesin loading in the absence of *IRC15* may not affect the maintenance of kinetochore–microtubule attachments.

The prefoldin complex is involved in sister chromatid cohesion

While *Irc15* promotes the loading of centromeric cohesin, its contribution to sister chromatid cohesion is unclear. Also unclear is whether the prefoldin complex affects this process. To examine this, we employed a strain in which a tandem LacO array was integrated 10 kb away from the *CEN4* locus and a LacR–GFP protein, which binds to the LacO array, is stably expressed (Fig. 4A). An increased number of G2/M cells with more than one GFP focus indicates a defect in sister chromatid cohesion in this strain (Fig. 4A,B). In our assays, a *kre1Δ* mutant defective in β-glucan assembly was included as a negative control, while *chl1Δ*, *bub1Δ* and *rts1Δ* mutants served as positive controls (Kitajima et al., 2005, 2006). As expected, two GFP foci were evident in ~10% of the *kre1Δ* cells in G2/M phase, which was comparable to that in WT cells (Fig. 4C, top). In contrast, at least ~20% of the *chl1Δ*, *bub1Δ* and *rts1Δ* cells displayed two GFP foci, indicative of a cohesion defect. Importantly, at least 20% of the *gim3Δ*, *gim4Δ*, *yke2Δ*, *pac10Δ* and *irc15Δ* cells showed more than two GFP foci, suggesting a defect in sister chromatid cohesion. It is noteworthy that an increased number of the prefoldin mutant cells also harbored two GFP spots in G1 phase. This may result from

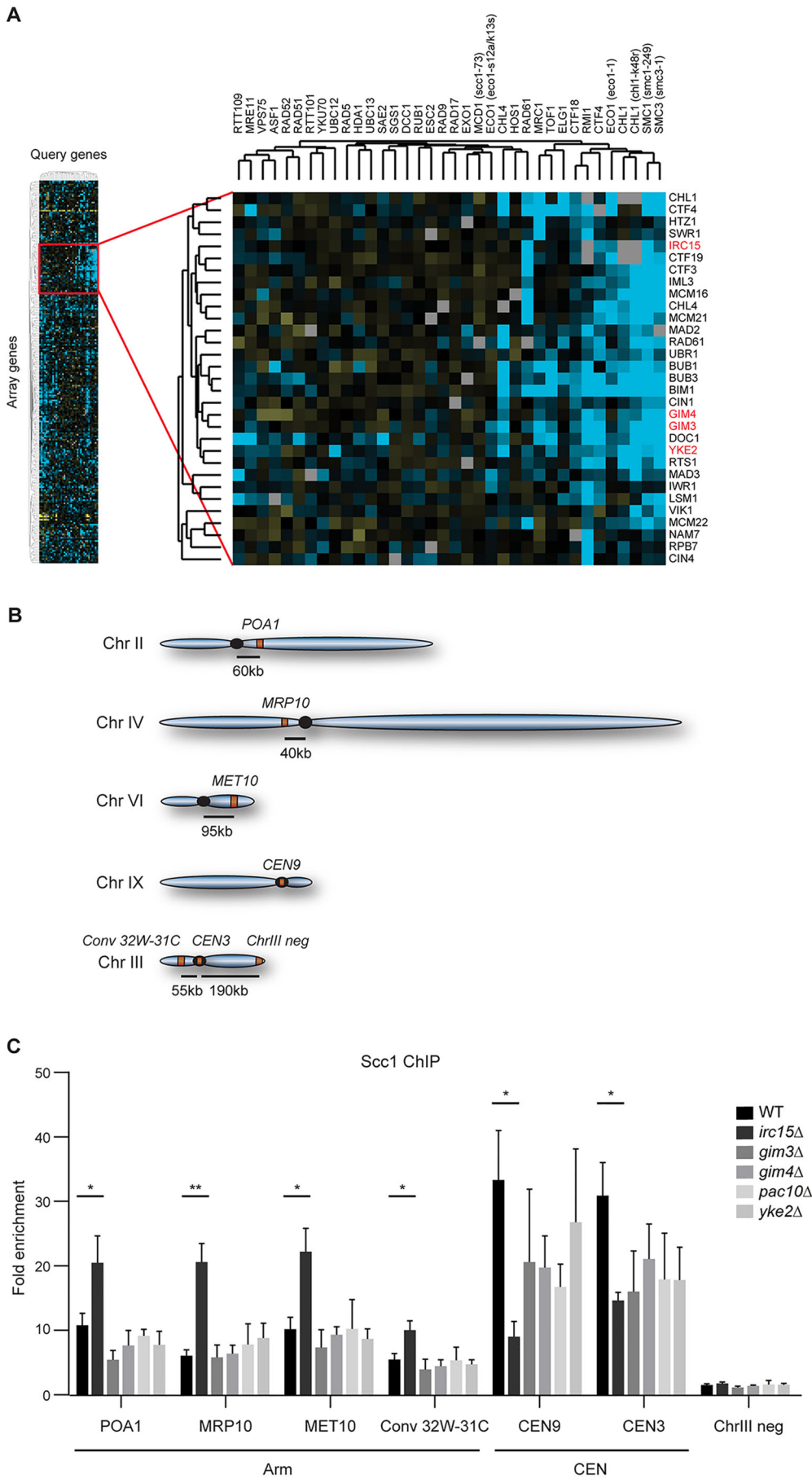


Fig. 3. Identification of new cohesin factors with *Irc15* as cohesin loader. (A) Heatmap displaying hierarchical clustering of genetic interactions scores (S-scores; left panel) identified a cluster of negative interactions involving cohesin factors and genes involved in chromosome segregation (right panel; blue, negative interaction; yellow, positive interaction; black, neutral interaction; gray, missing interaction). Potential new sister chromatid cohesion factors are highlighted in red. (B) Schematic of chromosomal loci assayed for *Scc1* loading. qPCR was performed at known cohesin binding sites either on centromeres (*CEN9* and *CEN3*) or genic (*POA1*, *MRP10* and *MET10*) and intergenic (*Conv 32W-31C*) regions on chromosome arms. *ChrIII neg* was a negative control. (C) Enrichment of *Scc1*-Myc assessed by ChIP-qPCR at the indicated loci in nocodazole-arrested strains. Enrichment corresponds to the ratio of the *Scc1*-Myc signal over that found with beads alone. Mean±s.e.m. enrichment for three (*gim3Δ*, *gim4Δ*, *yke2Δ* and *pac10Δ*) or four (WT, *irc15Δ*) independent experiments is shown. **P*<0.05; ***P*<0.01 (Student's *t*-test).

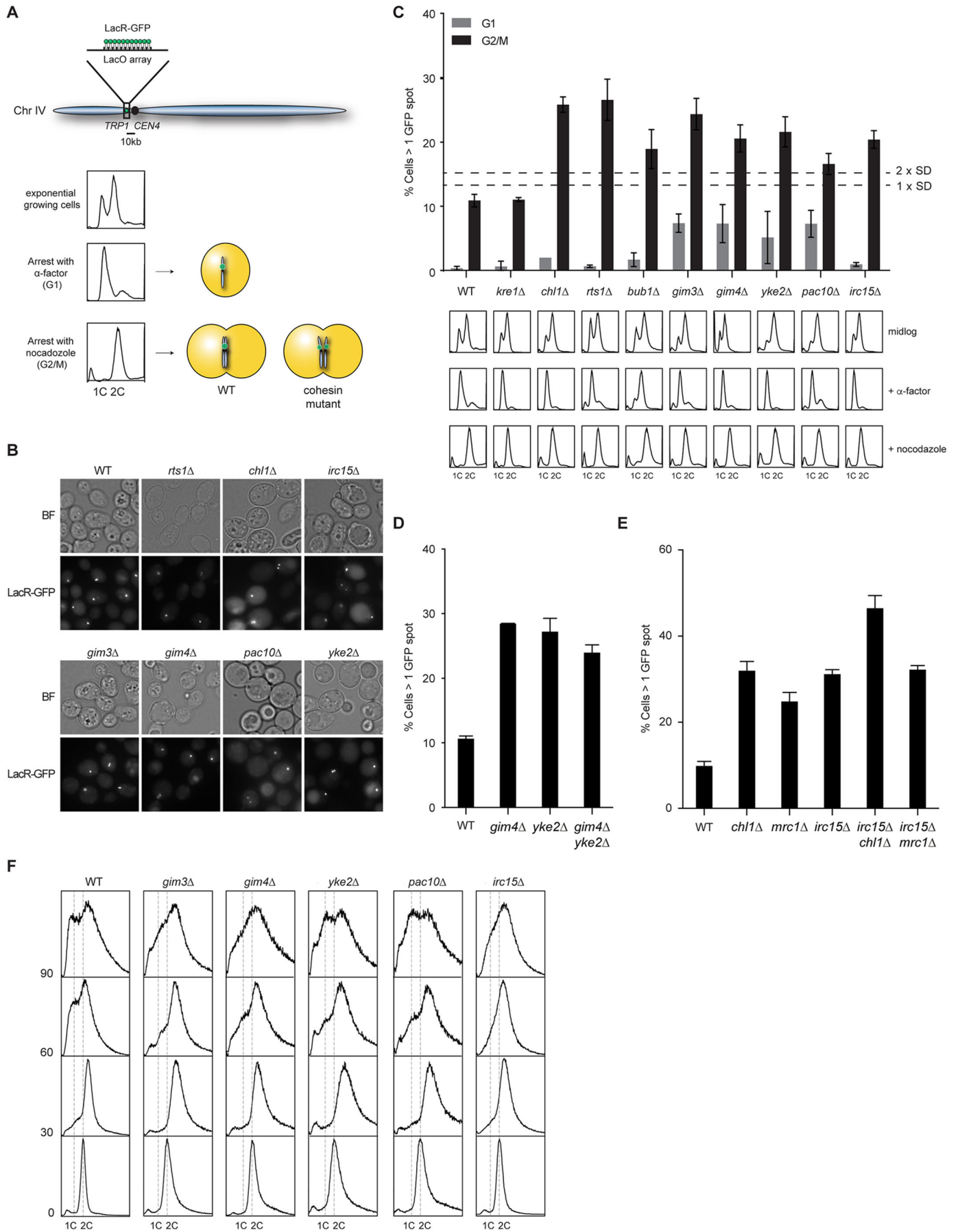


Fig. 4. See next page for legend.

Fig. 4. The prefoldin complex and *Irc15* affect cohesion establishment.

(A) Schematic of the sister chromatid cohesion assay. A LacO array was integrated on chromosome IV 10 kb away from *CEN4* in cells expressing the LacR–GFP fusion protein. Upon synchronization of the cells in G1 with α -factor or in G2/M with nocodazole, cells with normal sister chromatid cohesion show one spot in G1 and G2/M in the majority of the cells. Cohesin mutants show a larger fraction of cells with two GFP spots. (B) Representative images of the sister chromatid cohesion assay in nocodazole-arrested cells. (C) Quantification of sister chromatid cohesion in cells from B. The mean \pm s.e.m. percentage of cells with more than one GFP spot (top) is shown; \sim 400 cells were scored in at least three independent experiments for each strain. Flow cytometry analysis of DNA content was used to monitor cell synchronization (bottom). (D,E) Quantification of sister chromatid cohesion in the indicated cells as in B. (F) Flow cytometry analysis of M phase progression of the indicated strains. Cells were arrested in G2/M by nocodazole treatment, released in YPAD and analyzed at the indicated timepoints.

chromosome mis-segregation during the previous mitosis, which might be a consequence of defective cohesion (Hoque and Ishikawa, 2002; Sonoda et al., 2001), although we could not detect any aneuploidy in these mutants (Fig. 4C, bottom), likely due to the low frequency of these events (<10%). To determine whether the prefoldin holocomplex is involved in cohesion establishment, we compared sister chromatid cohesion in *gim4* Δ and *yke2* Δ single and double mutants (Fig. 4D). *gim4* Δ and *yke2* Δ were epistatic with regard to their cohesion defect, suggesting that the prefoldin complex as a whole functions in the same pathway for cohesion establishment. In addition, we also evaluated whether *Irc15* functions in one of the two parallel non-essential cohesion pathways or defines a new cohesion pathway (Xu et al., 2007). To this end, we generated double mutants of *IRC15* with *CHL1* or *MRC1*, which encode components of the cohesion pathways involving Csm3 and Ctf18–RFC, respectively (Xu et al., 2007). While *irc15* Δ was epistatic with *mrc1* Δ , it displayed additive cohesion defects with *chl1* Δ . These results suggest that *Irc15* functions with *Mrc1* in the cohesion pathway involving Ctf18–RFC. Finally, we compared the resumption of cell cycle progression of *irc15* Δ and the prefoldin mutants following a G2/M arrest. Although WT cells progressed through mitosis and started to enter G1 by 60 min, the majority of the *irc15* Δ and prefoldin mutant cells were still in mitosis at that time, showing a clear delay in cell cycle progression (Fig. 4F), consistent with a sister chromatid cohesion defect (Sonoda et al., 2001). Thus, we reveal that *Irc15* and the prefoldin complex promote efficient sister chromatid cohesion. While *Irc15* promotes this process, likely by facilitating the loading of centromeric cohesin, it is unclear how the prefoldin complex would affect this process. Given that prefoldin delivers unfolded proteins to cytosolic chaperonins (Vainberg et al., 1998), we checked whether it may affect the stability of the cohesin core subunits. However, *Smc1*, *Smc3*, *Sccl* and *Sccl3* stability remained unaffected in *gim3* Δ cells (Fig. S4).

DISCUSSION

Here, we generated a comprehensive genetic interaction network centered on cohesin comprising 373 genetic interactions specific for cohesin factors. The network uncovered novel connections for cohesin genes in various cellular processes. Moreover, it also revealed new factors involved in sister chromatid cohesion, namely the microtubule-associated protein *Irc15* and the prefoldin complex members *Gim3*, *Gim4* and *Yke2*. Thus, our genetic interaction map provides a unique resource for the further identification and functional interrogation of cohesin proteins.

Irc15 was initially identified in different screens that were designed to identify factors involved in chromosome segregation and DNA repair (Alvaro et al., 2007; Measday et al., 2005; Daniel

et al., 2006; Jordan et al., 2007). It was also shown that *Irc15* associates with microtubules, regulating their dynamics and mediating tension between kinetochores (Keyes and Burke, 2009). Here, we identified a novel role for *Irc15* in centromeric cohesin loading and cohesion establishment. Proper centromeric cohesion is a prerequisite to generate a dynamic tension between microtubules and sister chromatids in yeast (Goshima and Yanagida, 2000; He et al., 2000; Tanaka et al., 2000). This tension is also required for the establishment of stable microtubule–kinetochore attachments (Ault and Nicklas, 1989; Nicklas and Ward, 1994; Koshland et al., 1988; Skibbens et al., 1995). Indeed, loss of *Sccl* impairs both sister chromatid cohesion and kinetochore function in higher eukaryotes (Sonoda et al., 2001). However, in the case of *irc15* Δ our results suggest that the kinetochore defect did not result from the cohesin loading defect observed in this mutant background. Conversely, several inner and central kinetochore proteins play a role in the recruitment of pericentromeric cohesin (Eckert et al., 2007; Hinshaw et al., 2017). However, cells with defective microtubule–kinetochore attachments exhibit high levels of *Sccl* loading at centromeres (Eckert et al., 2007). Given that *Irc15* controls tension between kinetochores and microtubules (Keyes and Burke, 2009), and that we observed a decrease in centromeric cohesin loading in the absence of *IRC15*, it is unlikely that the cohesion defect in *irc15* Δ cells stems from a kinetochore defect. Rather, *Irc15* may play independent roles in cohesin loading and microtubule–kinetochore attachment at centromeres.

We also identified the prefoldin complex as a new factor involved in sister chromatid cohesion. The prefoldin complex is a multi-subunit chaperone that assists in the proper folding of proteins in the cytosol (Vainberg et al., 1998). Even though it did not affect the stability of the cohesin core subunits, it is tempting to speculate that prefoldin targets one or more (other) factors involved in sister chromatid cohesion, thereby affecting this process. Alternatively, the involvement of the prefoldin complex in cohesion might also be related to its role in regulating chromatin structure during transcription elongation (Millan-Zambrano et al., 2013). To this end, it may either influence the transcription of genes involved in cohesion or allow the loading of the cohesin complex by generating nucleosome-free regions at transcribed genes (Millan-Zambrano et al., 2013). This hypothesis is supported by our genetic interaction network, which identified a strong relationship between cohesin factors and factors involved in gene expression and/or chromatin remodeling. To this end, it is interesting to note that the RSC chromatin remodeling complex facilitates the association of cohesin on chromosome arms by generating a nucleosome-free region (Huang et al., 2004; Huang and Laurent, 2004; Munoz et al., 2019). Moreover, the SWR1 complex deposits the histone variant H2A.Z, whose acetylation helps to maintain sister chromatin cohesion (Sharma et al., 2013). Finally, it was also shown that the NAD⁺-dependent deacetylase Hst3, a member of the sirtuin superfamily, is involved in sister chromatid cohesion through the acetylation of histone H3 at lysine K56 (Thaminy et al., 2007), and that strains harboring mutations in cohesin genes are sensitive to sirtuin inhibitors (Choy et al., 2015). These findings may enforce a potential link between prefoldin and chromatin remodeling in cohesion establishment.

Among the novel connections for cohesin genes, we identified several interactions linked to post-replication repair and nucleotide excision repair. Further studies may reveal the functional importance of the link between sister chromatid cohesion and these processes. Since defects in nucleotide excision repair are associated with Cockayne syndrome and xeroderma pigmentosum, we anticipate that the link between cohesin factors and this repair

process may be relevant for disease etiology. In line with this, it was recently shown that the nucleotide excision repair structure-specific endonuclease ERCC1–XPF complex interacts with the cohesin complex and other proteins at promoters to silence imprinted genes during development in mice (Chatzinikolaou et al., 2017). Moreover, since sister chromatid cohesion and the factors involved are well conserved from yeast to men (Xiong and Gerton, 2010), our network may also inform on genetic interactions of cohesin factors mutated in cohesinopathies or cancer.

MATERIALS AND METHODS

Genetic interaction map analysis

The genetic interaction map was generated and analyzed as previously described (Srivastava et al., 2013). Briefly, an array of 1494 genes (Table S2) was collected from the yeast deletion collection (Mat-alpha) and the DAMP library containing a KANMX selection marker. To generate the query genes (Table S1), mutant strains carrying deletion mutations were generated by PCR gene targeting (Longtine et al., 1998), while mutants carrying point mutations were either generated using the MIRAGE method (Nair and Zhao, 2009) in a strain containing synthetic genetic array (SGA) anti-diploid selection markers and a NATMX selection marker, or by using strains obtained from Charles Boone (Donnelly Centre, University of Toronto, Canada) and Philip Hieter (Michael Smith Laboratories, University of British Columbia, Canada). Primers used to generate these mutants are available upon request. Owing to the presence of temperature-sensitive mutants, the generation of double mutants was performed at permissive temperature (23°C) with use of the SGA procedure in quadruplicate using the ROTOR HDA (Singer Instruments) pinning robot (Tong and Boone, 2006). Genetic interactions were assessed at semi-permissive temperature (30°C). Pictures were taken with a Canon Powershot G3. Colony sizes were quantified and normalized using Matlab Colony Analyzer (Bean et al., 2014). Quantitative S-scores were calculated using Matlab as previously described (Collins et al., 2010; Guenole et al., 2013). Network visualizations of genetic interactions were performed using Cytoscape (Shannon et al., 2003). The Cytoscape plugin BiNGO was used for GO term enrichment analysis (Maere et al., 2005). Unsupervised clustering was performed using Cluster 3.0 using a selection of array genes that show a magnitude of S-score > 2.0 in at least one of the query genes and a variation with a standard deviation > 0.8 in the query genes. The clustering was visualized in a heatmap using Java TreeView.

Yeast strains and culture conditions

A strain expressing 18Myc-tagged Scc1 and HA-tagged Pds1 was used in flow cytometry and Scc1-based ChIP experiments. PCR gene targeting was used to generate the tagged alleles and gene deletions (Table S8). A strain carrying a LacO array integrated on chromosome IV 10 kb away from *CEN4* and expressing a LacR–GFP fusion protein was used for sister chromatid cohesion assays (Shimada and Gasser, 2007). PCR gene targeting was used to generate gene deletions in this background (Table S8). Primers used to generate yeast strains are available upon request. All yeast strains were cultured in rich YPAD medium or Synthetic Complete medium lacking methionine (SC-methionine).

Chromatin immunoprecipitation

Chromatin immunoprecipitation (ChIP) was performed as previously described with slight modifications (Cobb et al., 2003). Briefly, cells were grown to 5×10^6 cells/ml in YPAD and synchronized in G2/M by incubation with nocodazole (7.5 µg/ml) for 2 h for Scc1 ChIP. Nocodazole (7.5 µg/ml) was added a second time after 1 h of incubation. Alternatively, cells were synchronized in G1 with α -factor for 2 h, washed and released in YPAD containing nocodazole for 0, 30, 60, 90 and 120 min. Samples were fixed with 1% formaldehyde. For Ndc80–GFP ChIP, cells were grown overnight in SC-methionine containing 2% raffinose, diluted and grown in the presence of 2% glucose or 2% galactose for 4 h, diluted to 5×10^6 cells/ml and fixed with 1% formaldehyde. Extracts were prepared in lysis buffer (50 mM Hepes, pH 7.5, 140 mM NaCl, 1 mM Na EDTA, 1% Triton X-100 and 0.1% sodium deoxycholate) containing protease inhibitors. Extracts were

subjected to immunoprecipitation with Dynabeads mouse or rabbit IgG (Invitrogen, M-280) coated with antibody against c-Myc (9B11, Cell Signaling) or GFP (ab290, Abcam). DNA was purified and enrichment at specific loci was measured by performing quantitative (q)PCR. Relative enrichment was determined by the $2^{-\Delta\Delta Ct}$ method (Livak and Schmittgen, 2001; Cobb and van Attekum, 2010). Dynabeads alone were used to correct for background. An amplicon 11 kb downstream of ARS305, devoid of Scc1 binding, was used for Scc1 ChIP normalization (Tittel-Elmer et al., 2012). An amplicon devoid of Ndc80 binding (Neg1p1) was used for Ndc80 ChIP normalization (Lefrançois et al., 2013). Primers used are listed in Table S9.

Sister chromatid cohesion assay

Sister chromatid cohesion was assayed using a strain containing a LacO repeat integrated at chromosome 4 between *ARS1* and *CEN4* at 10 kb distance to *CEN4* and a LacR–GFP expression cassette integrated at the *HIS3* locus (Shimada and Gasser, 2007). Cells were grown to mid-log phase in YPAD, synchronized in G1 by incubation with α -factor for 1.5 h, or in G2/M by incubation with nocodazole (15 µg/ml) for 1 h. Cells were fixed in 4% paraformaldehyde at room temperature for 15 min, washed and resuspended in KPO₄/Sorbitol solution (10 mM KPO₄, 1.2 M Sorbitol, pH 7.5). Images of cells were acquired on a Zeiss AxioImager M2 widefield fluorescence microscope equipped with 100× PLAN APO (1.4 NA) oil-immersion objectives (Zeiss) and an HXP 120 metal-halide lamp used for excitation. Fluorescence signals were detected using the following filters: GFP/YFP 488 (excitation filter: 470/40 nm, dichroic mirror: 495 nm, emission filter: 525/50 nm). Images were recorded and analyzed using ZEN 2012 software.

Flow cytometry

Cells were grown to midlog phase in YPAD, synchronized in G1 by incubation with α -factor for 1.5 h, or in G2/M by incubation with nocodazole (15 µg/ml) for 1 h. Alternatively, cells were grown to midlog phase in YPAD, synchronized in G2/M by incubation with nocodazole (15 µg/ml) for 2 h, washed and released in YPAD. Samples were prepared as previously described (Haase and Lew, 1997). Data were acquired on a BD FACSCalibur (BD Biosciences) or on a Novocyte (ACEA Biosciences, Inc) and analyzed with FlowJo or NovoExpress software, respectively.

Spot dilution test

Cells were grown overnight in YPAD and then plated in fivefold serial dilutions starting at a density of 6×10^6 cells/ml (OD_{600 nm} = 0.5) on YPAD plates. Cells were grown for 3 days at the semi-permissive temperature (30°C) before images were taken.

Cycloheximide chase experiment

Cells expressing Scc1–18Myc, Scc3–6FLAG, Smc1–6FLAG or Smc3–6FLAG (Table S8) were subjected to cycloheximide chase analysis as previously described (Buchanan et al., 2016). Samples were collected at 0, 30, 60 and 90 min after cycloheximide treatment. Whole-cell extracts were prepared by post-alkaline protein extraction and analyzed by SDS-PAGE. Western blotting was performed using an anti-c-Myc antibody (1:1000, 9E10, cat. no. sc-40, Santa Cruz Biotechnology) and FLAG antibody (1:5000, clone M2, cat. no. F1804, Sigma). Ponceau staining served as a loading control.

Curation of *S. cerevisiae*–*S. pombe* and *S. cerevisiae*–*H. sapiens* orthologs

Information about budding yeast-to-human and budding yeast-to-fission yeast orthologs was collected from two different sources, InParanoid (O'Brien et al., 2005) and PomBase (Lock et al., 2018), and is presented in Table S7. InParanoid inventories orthologs based on protein sequence similarity, whereas PomBase curates orthologs based on both function and sequence similarity.

Acknowledgements

We thank Charles Boone, Philip Hieter, Jennifer Cobb and Paul van Heusden for providing yeast strains, Gerda Lamers for microscopy assistance and Rohith Srivas for helping with the curation of orthologs.

Competing interests

The authors declare no competing or financial interests.

Author contributions

Conceptualization: S.M.S., H.v.A.; Methodology: S.M.S., A.B., T.I., F.v.L., H.v.A.; Software: S.M.S., G.B., T.I.; Validation: S.M.S., A.B., M.E., S.v.d.H.; Formal analysis: S.M.S., A.B., M.E., G.B.; Investigation: S.M.S., A.B., M.E., S.v.d.H., T.v.W.; Resources: F.v.L., H.v.A.; Data curation: S.M.S., A.B., M.E., S.v.d.H.; Writing - original draft: S.M.S., A.B.; Writing - review & editing: S.M.S., A.B., H.v.A.; Visualization: S.M.S., A.B., H.v.A.; Supervision: H.v.A.; Funding acquisition: T.I., F.v.L., H.v.A.

Funding

This work was financially supported by grants from the US National Institutes of Health (ES014811, GM103504) to G.B. and T.I., the Netherlands Organisation for Scientific Research (Nederlandse Organisatie voor Wetenschappelijk; NWO VICI-016.130.627) to F.v.L. and (NWO TOP-GO-85410013) to H.v.A., and the European Research Council (ERC Consolidator grant - 617485) to H.v.A. Deposited in PMC for immediate release.

Supplementary information

Supplementary information available online at <http://jcs.biologists.org/lookup/doi/10.1242/jcs.237628.supplemental>

Peer review history

The peer review history is available online at <https://jcs.biologists.org/lookup/doi/10.1242/jcs.237628.reviewer-comments.pdf>

References

- Alexandru, G., Zachariae, W., Schleiffer, A. and Nasmyth, K. (1999). Sister chromatid separation and chromosome re-duplication are regulated by different mechanisms in response to spindle damage. *EMBO J.* **18**, 2707-2721. doi:10.1093/emboj/18.10.2707
- Alvaro, D., Lisby, M. and Rothstein, R. (2007). Genome-wide analysis of Rad52 foci reveals diverse mechanisms impacting recombination. *PLoS Genet* **3**, e228. doi:10.1371/journal.pgen.0030228
- Ault, J. G. and Nicklas, R. B. (1989). Tension, microtubule rearrangements, and the proper distribution of chromosomes in mitosis. *Chromosoma* **98**, 33-39. doi:10.1007/BF00293332
- Bailey, M. L., O'neil, N. J., Van Pel, D. M., Solomon, D. A., Waldman, T. and Hieter, P. (2014). Glioblastoma cells containing mutations in the cohesin component STAG2 are sensitive to PARP inhibition. *Mol. Cancer Ther.* **13**, 724-732. doi:10.1158/1535-7163.MCT-13-0749
- Bean, G. J., Jaeger, P. A., Bahr, S. and Ideker, T. (2014). Development of ultra-high-density screening tools for microbial "omics". *PLoS One* **9**, e85177. doi:10.1371/journal.pone.0085177
- Ben-Aroya, S., Koren, A., Liefshitz, B., Steinlauf, R. and Kupiec, M. (2003). ELG1, a yeast gene required for genome stability, forms a complex related to replication factor C. *Proc. Natl. Acad. Sci. USA* **100**, 9906-9911. doi:10.1073/pnas.1633757100
- Boginya, A., Detroja, R., Matityahu, A., Frenkel-Morgenstern, M. and Onn, I. (2019). The chromatin remodeler Chd1 regulates cohesin in budding yeast and humans. *Sci. Rep.* **9**, 8929. doi:10.1038/s41598-019-45263-3
- Bose, T., Lee, K. K., Lu, S., Xu, B., Harris, B., Slaughter, B., Unruh, J., Garrett, A., Mcdowell, W., Box, A. et al. (2012). Cohesin proteins promote ribosomal RNA production and protein translation in yeast and human cells. *PLoS Genet* **8**, e1002749. doi:10.1371/journal.pgen.1002749
- Buchanan, B. W., Lloyd, M. E., Engle, S. M. and Rubenstein, E. M. (2016). Cycloheximide chase analysis of protein degradation in *Saccharomyces cerevisiae*. *J. Vis. Exp.* **110**, e53975. doi:10.3791/53975
- Chang, M., Bellaoui, M., Zhang, C., Desai, R., Morozov, P., Delgado-Cruzata, L., Rothstein, R., Freyer, G. A., Boone, C. and Brown, G. W. (2005). RMI1/NCE4, a suppressor of genome instability, encodes a member of the RecQ helicase/Topo III complex. *EMBO J.* **24**, 2024-2033. doi:10.1038/sj.emboj.7600684
- Chatzinikolaou, G., Apostolou, Z., Aid-Pavlidis, T., Ioannidou, A., Karakasilioti, I., Papadopoulos, G. L., Aivaliotis, M., Tsekrekou, M., Strouboulis, J., Kosteas, T. et al. (2017). ERCC1-XPF cooperates with CTCF and cohesin to facilitate the developmental silencing of imprinted genes. *Nat. Cell Biol.* **19**, 421-432. doi:10.1038/ncb3499
- Chen, Z., Mccrosky, S., Guo, W., Li, H. and Gerton, J. L. (2012). A genetic screen to discover pathways affecting cohesin function in *Schizosaccharomyces pombe* identifies chromatin effectors. *G3 (Bethesda)* **2**, 1161-1168. doi:10.1534/g3.112.003327
- Choy, J. S., Qadri, B., Henry, L., Shroff, K., Bifarin, O. and Basrai, M. A. (2015). A genome-wide screen with nicotinamide to identify sirtuin-dependent pathways in *saccharomyces cerevisiae*. *G3 (Bethesda)* **6**, 485-494. doi:10.1534/g3.115.022244
- Cobb, J. and Van Attikum, H. (2010). Mapping genomic targets of DNA helicases by chromatin immunoprecipitation in *Saccharomyces cerevisiae*. *Methods Mol. Biol.* **587**, 113-126. doi:10.1007/978-1-60327-355-8_8
- Cobb, J. A., Bjergbaek, L., Shimada, K., Frei, C. and Gasser, S. M. (2003). DNA polymerase stabilization at stalled replication forks requires Mec1 and the RecQ helicase Sgs1. *EMBO J.* **22**, 4325-4336. doi:10.1093/emboj/cdg391
- Cohen-Fix, O., Peters, J. M., Kirschner, M. W. and Koshland, D. (1996). Anaphase initiation in *Saccharomyces cerevisiae* is controlled by the APC-dependent degradation of the anaphase inhibitor Pds1p. *Genes Dev.* **10**, 3081-3093. doi:10.1101/gad.10.24.3081
- Collins, S. R., Roguev, A. and Krogan, N. J. (2010). Quantitative genetic interaction mapping using the E-MAP approach. *Methods Enzymol.* **470**, 205-231. doi:10.1016/S0076-6879(10)70009-4
- Costanzo, M., Baryshnikova, A., Bellay, J., Kim, Y., Spear, E. D., Sevier, C. S., Ding, H., Koh, J. L., Toufighi, K., Mostafavi, S. et al. (2010). The Genetic Landscape of a Cell. *Science* **327**, 425-431. doi:10.1126/science.1180823
- Costanzo, M., Kuzmin, E., Van Leeuwen, J., Mair, B., Moffat, J., Boone, C. and Andrews, B. (2019). Global genetic networks and the genotype-to-phenotype relationship. *Cell* **177**, 85-100. doi:10.1016/j.cell.2019.01.033
- Daniel, J. A., Keyes, B. E., Ng, Y. P., Freeman, C. O. and Burke, D. J. (2006). Diverse functions of spindle assembly checkpoint genes in *Saccharomyces cerevisiae*. *Genetics* **172**, 53-65. doi:10.1534/genetics.105.046441
- Deardorff, M. A., Bando, M., Nakato, R., Watrin, E., Itoh, T., Minamino, M., Saitoh, K., Komata, M., Katou, Y., Clark, D. et al. (2012). HDAC8 mutations in Cornelia de Lange syndrome affect the cohesin acetylation cycle. *Nature* **489**, 313-317. doi:10.1038/nature11316
- Deb, S., Xu, H., Tuynman, J., George, J., Yan, Y., Li, J., Ward, R. L., Mortensen, N., Hawkins, N. J., Mckay, M. J. et al. (2014). RAD21 cohesin overexpression is a prognostic and predictive marker exacerbating poor prognosis in KRAS mutant colorectal carcinomas. *Br. J. Cancer* **110**, 1606-1613. doi:10.1038/bjc.2014.31
- Dorsett, D. (2011). Cohesin: genomic insights into controlling gene transcription and development. *Curr. Opin. Genet. Dev.* **21**, 199-206. doi:10.1016/j.gde.2011.01.018
- Eckert, C. A., Gravidahl, D. J. and Megee, P. C. (2007). The enhancement of pericentromeric cohesin association by conserved kinetochore components promotes high-fidelity chromosome segregation and is sensitive to microtubule-based tension. *Genes Dev.* **21**, 278-291. doi:10.1101/gad.1498707
- Edwards, S., Li, C. M., Levy, D. L., Brown, J., Snow, P. M. and Campbell, J. L. (2003). *Saccharomyces cerevisiae* DNA polymerase epsilon and polymerase sigma interact physically and functionally, suggesting a role for polymerase epsilon in sister chromatid cohesion. *Mol. Cell Biol.* **23**, 2733-2748. doi:10.1128/MCB.23.8.2733-2748.2003
- Fernius, J. and Marston, A. L. (2009). Establishment of cohesion at the pericentromere by the Ctf19 kinetochore subcomplex and the replication fork-associated factor, Csm3. *PLoS Genet.* **5**, e1000629. doi:10.1371/journal.pgen.1000629
- Garg, R., Callens, S., Lim, D. S., Canman, C. E., Kastan, M. B. and Xu, B. (2004). Chromatin association of rad17 is required for an ataxia telangiectasia and rad-related kinase-mediated S-phase checkpoint in response to low-dose ultraviolet radiation. *Mol. Cancer Res.* **2**, 362-369.
- Gelot, C., Guirouilh-Barbat, J., Le Guen, T., Dardillac, E., Chailleux, C., Canitrot, Y. and Lopez, B. S. (2016). The cohesin complex prevents the end joining of distant DNA double-strand ends. *Mol. Cell* **61**, 15-26. doi:10.1016/j.molcel.2015.11.002
- Goshima, G. and Yanagida, M. (2000). Establishing biorientation occurs with precocious separation of the sister kinetochores, but not the arms, in the early spindle of budding yeast. *Cell* **100**, 619-633. doi:10.1016/S0092-8674(00)80699-6
- Guenole, A., Srivas, R., Vreeken, K., Wang, Z. Z., Wang, S., Krogan, N. J., Ideker, T. and Van Attikum, H. (2013). Dissection of DNA damage responses using multidimensional genetic interaction maps. *Mol. Cell* **49**, 346-358. doi:10.1016/j.molcel.2012.11.023
- Gullerova, M. and Proudfoot, N. J. (2008). Cohesin complex promotes transcriptional termination between convergent genes in *S. pombe*. *Cell* **132**, 983-995. doi:10.1016/j.cell.2008.02.040
- Haase, S. B. and Lew, D. J. (1997). Flow cytometric analysis of DNA content in budding yeast. *Methods Enzymol.* **283**, 322-332. doi:10.1016/S0076-6879(97)83026-1
- Hanna, J. S., Kroll, E. S., Lundblad, V. and Spencer, F. A. (2001). *Saccharomyces cerevisiae* CTF18 and CTF4 are required for sister chromatid cohesion. *Mol. Cell Biol.* **21**, 3144-3158. doi:10.1128/MCB.21.9.3144-3158.2001
- Harris, B., Bose, T., Lee, K. K., Wang, F., Lu, S., Ross, R. T., Zhang, Y., French, S. L., Beyer, A. L., Slaughter, B. D. et al. (2014). Cohesion promotes nucleolar structure and function. *Mol. Biol. Cell* **25**, 337-346. doi:10.1091/mbc.e13-07-0377
- Hartman, J. L. T., Garvik, B. and Hartwell, L. (2001). Principles for the buffering of genetic variation. *Science* **291**, 1001-1004. doi:10.1126/science.291.5506.1001
- He, X., Asthana, S. and Sorger, P. K. (2000). Transient sister chromatid separation and elastic deformation of chromosomes during mitosis in budding yeast. *Cell* **101**, 763-775. doi:10.1016/S0092-8674(00)80888-0
- Heidinger-Pauli, J. M., Únal, E. and Koshland, D. (2009). Distinct targets of the Eco1 acetyltransferase modulate cohesion in S phase and in response to DNA damage. *Mol. Cell* **34**, 311-321. doi:10.1016/j.molcel.2009.04.008

- Hinshaw, S. M., Makrantonis, V., Harrison, S. C. and Marston, A. L. (2017). The kinetochore receptor for the cohesin loading complex. *Cell* **171**, 72–84. doi:10.1016/j.cell.2017.08.017
- Hoque, M. T. and Ishikawa, F. (2002). Cohesin defects lead to premature sister chromatid separation, kinetochore dysfunction, and spindle-assembly checkpoint activation. *J. Biol. Chem.* **277**, 42306–42314. doi:10.1074/jbc.M206836200
- Huang, J., Hsu, J. M. and Laurent, B. C. (2004). The RSC nucleosome-remodeling complex is required for Cohesin's association with chromosome arms. *Mol. Cell* **13**, 739–750. doi:10.1016/S1097-2765(04)00103-0
- Huang, J. and Laurent, B. C. (2004). A Role for the RSC chromatin remodeler in regulating cohesion of sister chromatid arms. *Cell Cycle* **3**, 973–975. doi:10.4161/cc.3.8.1014
- Jordan, P. W., Klein, F. and Leach, D. R. (2007). Novel roles for selected genes in meiotic DNA processing. *PLoS Genet* **3**, e222. doi:10.1371/journal.pgen.0030222
- Kanellis, P., Agyei, R. and Durocher, D. (2003). Elg1 forms an alternative PCNA-interacting RFC complex required to maintain genome stability. *Curr. Biol.* **13**, 1583–1595. doi:10.1016/S0960-9822(03)00578-5
- Keys, B. E. and Burke, D. J. (2009). Irc15 is a microtubule-associated protein that regulates microtubule dynamics in *Saccharomyces cerevisiae*. *Curr. Biol.* **19**, 472–478. doi:10.1016/j.cub.2009.01.068
- Kim, S. T., Xu, B. and Kastan, M. B. (2002). Involvement of the cohesin protein, Smc1, in Atm-dependent and independent responses to DNA damage. *Genes Dev.* **16**, 560–570. doi:10.1101/gad.970602
- Kitajima, T. S., Hauf, S., Ohsugi, M., Yamamoto, T. and Watanabe, Y. (2005). Human Bub1 defines the persistent cohesion site along the mitotic chromosome by affecting Shugoshin localization. *Curr. Biol.* **15**, 353–359. doi:10.1016/j.cub.2004.12.044
- Kitajima, T. S., Sakuno, T., Ishiguro, K., Iemura, S., Natsume, T., Kawashima, S. A. and Watanabe, Y. (2006). Shugoshin collaborates with protein phosphatase 2A to protect cohesin. *Nature* **441**, 46–52. doi:10.1038/nature04663
- Kong, X., Ball, A. R., Jr, Pham, H. X., Zeng, W., Chen, H. Y., Schmiesing, J. A., Kim, J. S., Berns, M. and Yokomori, K. (2014). Distinct functions of human cohesin-SA1 and cohesin-SA2 in double-strand break repair. *Mol. Cell Biol.* **34**, 685–698. doi:10.1128/MCB.01503-13
- Koshland, D. E., Mitchison, T. J. and Kirschner, M. W. (1988). Polewards chromosome movement driven by microtubule depolymerization in vitro. *Nature* **331**, 499–504. doi:10.1038/331499a0
- Lefrançois, P., Auerbach, R. K., Yellman, C. M., Roeder, G. S. and Snyder, M. (2013). Centromere-like regions in the budding yeast genome. *PLoS Genet* **9**, e1003209. doi:10.1371/journal.pgen.1003209
- Lengronne, A., Katou, Y., Mori, S., Yokobayashi, S., Kelly, G. P., Itoh, T., Watanabe, Y., Shirahige, K. and Uhlmann, F. (2004). Cohesin relocation from sites of chromosomal loading to places of convergent transcription. *Nature* **430**, 573–578. doi:10.1038/nature02742
- Lengronne, A. and Schwob, E. (2002). The yeast CDK inhibitor Sic1 prevents genomic instability by promoting replication origin licensing in late G(1). *Mol. Cell* **9**, 1067–1078. doi:10.1016/S1097-2765(02)00513-0
- Liu, J. and Baynam, G. (2010). Cornelia de Lange syndrome. *Adv. Exp. Med. Biol.* **685**, 111–123. doi:10.1007/978-1-4419-6448-9_11
- Livak, K. J. and Schmittgen, T. D. (2001). Analysis of relative gene expression data using real-time quantitative PCR and the 2(-Delta Delta C(T)) method. *Methods* **25**, 402–408. doi:10.1006/meth.2001.1262
- Lock, A., Rutherford, K., Harris, M. A. and Wood, V. (2018). PomBase: the scientific resource for fission yeast. *Methods Mol. Biol.* **1757**, 49–68. doi:10.1007/978-1-4939-7737-6_4
- Longtine, M. S., Mckenzie, A., III, Demarini, D. J., Shah, N. G., Wach, A., Brachat, A., Philippsen, P. and Pringle, J. R. (1998). Additional modules for versatile and economical PCR-based gene deletion and modification in *Saccharomyces cerevisiae*. *Yeast* **14**, 953–961. doi:10.1080/0893-4648.1998.10012502
- Lu, S., Lee, K. K., Harris, B., Xiong, B., Bose, T., Saraf, A., Hattem, G., Florens, L., Seidel, C. and Gerton, J. L. (2014). The cohesin acetyltransferase Eco1 coordinates rDNA replication and transcription. *EMBO Rep.* **15**, 609–617. doi:10.1002/embr.201337974
- Maere, S., Heymans, K. and Kuiper, M. (2005). BINGO: a Cytoscape plugin to assess overrepresentation of gene ontology categories in biological networks. *Bioinformatics* **21**, 3448–3449. doi:10.1093/bioinformatics/bti551
- Mani, R., St Onge, R. P., Hartman, J. L. T., Giaever, G. and Roth, F. P. (2008). Defining genetic interaction. *Proc. Natl. Acad. Sci. USA* **105**, 3461–3466. doi:10.1073/pnas.0712255105
- Mayer, M. L., Pot, I., Chang, M., Xu, H., Aneliunas, V., Kwok, T., Newitt, R., Aebersold, R., Boone, C., Brown, G. W. et al. (2004). Identification of protein complexes required for efficient sister chromatid cohesion. *Mol. Biol. Cell* **15**, 1736–1745. doi:10.1091/mbc.e03-08-0619
- McAleenan, A., Clemente-Blanco, A., Cordon-Preciado, V., Sen, N., Esteras, M., Jarmuz, A. and Aragon, L. (2013). Post-replicative repair involves separate-dependent removal of the kleisin subunit of cohesin. *Nature* **493**, 250–254. doi:10.1038/nature11630
- McClelland, M. L., Gardner, R. D., Kallio, M. J., Daum, J. R., Gorbisky, G. J., Burke, D. J. and Stukenberg, P. T. (2003). The highly conserved Ndc80 complex is required for kinetochore assembly, chromosome congression, and spindle checkpoint activity. *Genes Dev.* **17**, 101–114. doi:10.1101/gad.1040903
- McLellan, J. L., O'neil, N. J., Barrett, I., Ferree, E., Van Pel, D. M., Ushey, K., Sipahimalani, P., Bryan, J., Rose, A. M. and Hieter, P. (2012). Synthetic lethality of cohesins with PARPs and replication fork mediators. *PLoS Genet* **8**, e1002574. doi:10.1371/journal.pgen.1002574
- Measday, V., Baetz, K., Guzzo, J., Yuen, K., Kwok, T., Sheikh, B., Ding, H., Ueta, R., Hoac, T., Cheng, B. et al. (2005). Systematic yeast synthetic lethal and synthetic dosage lethal screens identify genes required for chromosome segregation. *Proc. Natl. Acad. Sci. USA* **102**, 13956–13961. doi:10.1073/pnas.0503504102
- Michaelis, C., Ciosk, R. and Nasmyth, K. (1997). Cohesins: chromosomal proteins that prevent premature separation of sister chromatids. *Cell* **91**, 35–45. doi:10.1016/S0092-8674(01)80007-6
- Millan-Zambrano, G., Rodriguez-Gil, A., Penate, X., De Miguel-Jimenez, L., Morillo-Huesca, M., Krogan, N. and Chavez, S. (2013). The prefoldin complex regulates chromatin dynamics during transcription elongation. *PLoS Genet* **9**, e1003776. doi:10.1371/journal.pgen.1003776
- Munoz, S., Minamino, M., Casas-Delucchi, C. S., Patel, H. and Uhlmann, F. (2019). A role for chromatin remodeling in cohesin loading onto chromosomes. *Mol. Cell* **74**, 664–673.e5. doi:10.1016/j.molcel.2019.02.027
- Nagao, K., Adachi, Y. and Yanagida, M. (2004). Separase-mediated cleavage of cohesin at interphase is required for DNA repair. *Nature* **430**, 1044–1048. doi:10.1038/nature02803
- Nair, N. U. and Zhao, H. (2009). Mutagenic inverted repeat assisted genome engineering (MIRAGE). *Nucleic Acids Res.* **37**, e9. doi:10.1093/nar/gkn943
- Nicklas, R. B. and Ward, S. C. (1994). Elements of error correction in mitosis: microtubule capture, release, and tension. *J. Cell Biol.* **126**, 1241–1253. doi:10.1083/jcb.126.5.1241
- O'brien, K. P., Remm, M. and Sonnhammer, E. L. (2005). Inparanoid: a comprehensive database of eukaryotic orthologs. *Nucleic Acids Res.* **33**, D476–D480. doi:10.1093/nar/gki107
- Pal, S., Postnikoff, S. D., Chavez, M. and Tyler, J. K. (2018). Impaired cohesion and homologous recombination during replicative aging in budding yeast. *Sci. Adv.* **4**, eaaq0236. doi:10.1126/sciadv.aag0236
- Parnas, O., Zipin-Roitman, A., Mazor, Y., Liefshitz, B., Ben-Aroya, S. and Kupiec, M. (2009). The ELG1 clamp loader plays a role in sister chromatid cohesion. *PLoS ONE* **4**, e5497. doi:10.1371/journal.pone.0005497
- Petronczki, M., Chwalla, B., Siomos, M. F., Yokobayashi, S., Helmhart, W., Deutschbauer, A. M., Davis, R. W., Watanabe, Y. and Nasmyth, K. (2004). Sister-chromatid cohesion mediated by the alternative RF-CCtf18/Dcc1/Ctf8, the helicase Chl1 and the polymerase-alpha-associated protein Ctf4 is essential for chromatid disjunction during meiosis II. *J. Cell Sci.* **117**, 3547–3559. doi:10.1242/jcs.01231
- Repo, H., Löytyniemi, E., Nykänen, M., Lintunen, M., Karra, H., Pitkanen, R., Söderström, M., Kuopio, T. and Kronqvist, P. (2016). The expression of cohesin subunit SA2 predicts breast cancer survival. *Appl. Immunohistochem. Mol. Morphol.* **24**, 615–621. doi:10.1097/PAI.0000000000000240
- Shannon, P., Markiel, A., Ozier, O., Baliga, N. S., Wang, J. T., Ramage, D., Amin, N., Schwikowski, B. and Ideker, T. (2003). Cytoscape: a software environment for integrated models of biomolecular interaction networks. *Genome Res.* **13**, 2498–2504. doi:10.1101/gr.1239303
- Sharma, U., Stefanova, D. and Holmes, S. G. (2013). Histone variant H2A.Z functions in sister chromatid cohesion in *Saccharomyces cerevisiae*. *Mol. Cell Biol.* **33**, 3473–3481. doi:10.1128/MCB.00162-12
- Shimada, K. and Gasser, S. M. (2007). The origin recognition complex functions in sister-chromatid cohesion in *Saccharomyces cerevisiae*. *Cell* **128**, 85–99. doi:10.1016/j.cell.2006.11.045
- Skibbens, R. V. (2004). Chl1p, a DNA helicase-like protein in budding yeast, functions in sister-chromatid cohesion. *Genetics* **166**, 33–42. doi:10.1534/genetics.166.1.33
- Skibbens, R. V., Rieder, C. L. and Salmon, E. D. (1995). Kinetochore motility after severing between sister centromeres using laser microsurgery: evidence that kinetochore directional instability and position is regulated by tension. *J. Cell Sci.* **108**, 2537–2548.
- Sonoda, E., Matsusaka, T., Morrison, C., Vagnarelli, P., Hoshi, O., Ushiki, T., Nojima, K., Fukagawa, T., Waizenegger, I. C., Peters, J. M. et al. (2001). Scc1/Rad21/Mcd1 is required for sister chromatid cohesion and kinetochore function in vertebrate cells. *Dev. Cell* **1**, 759–770. doi:10.1016/S1534-5807(01)00088-0
- Srivastava, R., Costelloe, T., Carvunis, A. R., Sarkar, S., Malta, E., Sun, S. M., Pool, M., Licon, K., Van Welsem, T., Van Leeuwen, F. et al. (2013). A UV-induced genetic network links the RSC complex to nucleotide excision repair and shows dose-dependent rewiring. *Cell Rep.* **5**, 1714–1724. doi:10.1016/j.celrep.2013.11.035
- St Onge, R. P., Mani, R., Oh, J., Proctor, M., Fung, E., Davis, R. W., Nislow, C., Roth, F. P. and Giaever, G. (2007). Systematic pathway analysis using high-resolution fitness profiling of combinatorial gene deletions. *Nat. Genet.* **39**, 199–206. doi:10.1038/ng1948

- Strom, L., Lindroos, H. B., Shirahige, K. and Sjogren, C.** (2004). Postreplicative recruitment of cohesin to double-strand breaks is required for DNA repair. *Mol. Cell* **16**, 1003-1015. doi:10.1016/j.molcel.2004.11.026
- Sun, X., Chen, H., Deng, Z., Hu, B., Luo, H., Zeng, X., Han, L., Cai, G. and Ma, L.** (2015). The Warsaw breakage syndrome-related protein DDX11 is required for ribosomal RNA synthesis and embryonic development. *Hum. Mol. Genet.* **24**, 4901-4915. doi:10.1093/hmg/ddv213
- Tanaka, T., Fuchs, J., Loidl, J. and Nasmyth, K.** (2000). Cohesin ensures bipolar attachment of microtubules to sister centromeres and resists their precocious separation. *Nat. Cell Biol.* **2**, 492-499. doi:10.1038/35019529
- Thaminy, S., Newcomb, B., Kim, J., Gatbonton, T., Foss, E., Simon, J. and Bedalov, A.** (2007). Hst3 is regulated by Mec1-dependent proteolysis and controls the S phase checkpoint and sister chromatid cohesion by deacetylating histone H3 at lysine 56. *J. Biol. Chem.* **282**, 37805-37814. doi:10.1074/jbc.M706384200
- Thol, F., Bollin, R., Gehlhaar, M., Walter, C., Dugas, M., Suchanek, K. J., Kirchner, A., Huang, L., Chaturvedi, A., Wichmann, M. et al.** (2014). Mutations in the cohesin complex in acute myeloid leukemia: clinical and prognostic implications. *Blood* **123**, 914-920. doi:10.1182/blood-2013-07-518746
- Tittel-Elmer, M., Lengronne, A., Davidson, M. B., Bacal, J., Francois, P., Hohl, M., Petrini, J. H. J., Pasero, P. and Cobb, J. A.** (2012). Cohesin association to replication sites depends on rad50 and promotes fork restart. *Mol. Cell* **48**, 98-108. doi:10.1016/j.molcel.2012.07.004
- Tong, A. H. and Boone, C.** (2006). Synthetic genetic array analysis in *Saccharomyces cerevisiae*. *Methods Mol. Biol.* **313**, 171-192. doi:10.1385/1-59259-958-3:171
- Uhlmann, F., Lottspeich, F. and Nasmyth, K.** (1999). Sister-chromatid separation at anaphase onset is promoted by cleavage of the cohesin subunit Scc1. *Nature* **400**, 37-42. doi:10.1038/21831
- Unal, E., Arbel-Eden, A., Sattler, U., Shroff, R., Lichten, M., Haber, J. E. and Koshland, D.** (2004). DNA damage response pathway uses histone modification to assemble a double-strand break-specific cohesin domain. *Mol. Cell* **16**, 991-1002. doi:10.1016/j.molcel.2004.11.027
- Unal, E., Heidinger-Pauli, J. M. and Koshland, D.** (2007). DNA double-strand breaks trigger genome-wide sister-chromatid cohesion through Eco1 (Ctf7). *Science* **317**, 245-248. doi:10.1126/science.1140637
- Vainberg, I. E., Lewis, S. A., Rommelaere, H., Ampe, C., Vandekerckhove, J., Klein, H. L. and Cowan, N. J.** (1998). Prefoldin, a chaperone that delivers unfolded proteins to cytosolic chaperonin. *Cell* **93**, 863-873. doi:10.1016/S0092-8674(00)81446-4
- Van Der Lelij, P., Chrzanowska, K. H., Godthelp, B. C., Rooimans, M. A., Oostra, A. B., Stumm, M., Zdzienicka, M. Z., Joenje, H. and De Winter, J. P.** (2010). Warsaw breakage syndrome, a cohesinopathy associated with mutations in the XPD helicase family member DDX11/ChIR1. *Am. J. Hum. Genet.* **86**, 262-266. doi:10.1016/j.ajhg.2010.01.008
- Vega, H., Waisfisz, Q., Gordillo, M., Sakai, N., Yanagihara, I., Yamada, M., Van Gosliga, D., Kayserili, H., Xu, C., Ozono, K. et al.** (2005). Roberts syndrome is caused by mutations in ESCO2, a human homolog of yeast ECO1 that is essential for the establishment of sister chromatid cohesion. *Nat. Genet.* **37**, 468-470. doi:10.1038/ng1548
- Warren, C. D., Eckley, D. M., Lee, M. S., Hanna, J. S., Hughes, A., Peyser, B., Jie, C., Irizarry, R. and Spencer, F. A.** (2004). S-phase checkpoint genes safeguard high-fidelity sister chromatid cohesion. *Mol. Biol. Cell* **15**, 1724-1735. doi:10.1091/mbc.e03-09-0637
- Wu, N., Kong, X., Ji, Z., Zeng, W., Potts, P. R., Yokomori, K. and Yu, H.** (2012). Scc1 sumoylation by Mms21 promotes sister chromatid recombination through counteracting Wapl. *Genes Dev.* **26**, 1473-1485. doi:10.1101/gad.193615.112
- Xiong, B. and Gerton, J. L.** (2010). Regulators of the cohesin network. *Annu. Rev. Biochem.* **79**, 131-153. doi:10.1146/annurev-biochem-061708-092640
- Xu, B., Lu, S. and Gerton, J. L.** (2014). Roberts syndrome: a deficit in acetylated cohesin leads to nucleolar dysfunction. *Rare Dis.* **2**, e27743. doi:10.4161/rdis.27743
- Xu, H., Boone, C. and Brown, G. W.** (2007). Genetic dissection of parallel sister-chromatid cohesion pathways. *Genetics* **176**, 1417-1429. doi:10.1534/genetics.107.072876
- Xu, H., Boone, C. and Klein, H. L.** (2004). Mrc1 is required for sister chromatid cohesion to aid in recombination repair of spontaneous damage. *Mol. Cell Biol.* **24**, 7082-7090. doi:10.1128/MCB.24.16.7082-7090.2004
- Yamin, K., Assa, M., Matityahu, A. and Onn, I.** (2020). Analyzing chromosome condensation in yeast by second-harmonic generation microscopy. *Curr. Genet.* **66**, 437-443. doi:10.1007/s00294-019-01034-1
- Zhang, J., Shi, D., Li, X., Ding, L., Tang, J., Liu, C., Shirahige, K., Cao, Q. and Lou, H.** (2017). Rtt101-Mms1-Mms22 coordinates replication-coupled sister chromatid cohesion and nucleosome assembly. *EMBO Rep.* **18**, 1294-1305. doi:10.15252/embr.201643807